V European Conference on Computational Fluid Dynamics
ECCOMAS CFD 2010
J. C. F. Pereira and A. Sequeira (Eds)
Lisbon, Portugal,14-17 June 2010

LES MODELING OF KINETICS-CONTROLLED COMBUSTION REGIMES: AUTOIGNITION

Matthias Ihme and Yee Chee See

Department of Aerospace Engineering
University of Michigan, Ann Arbor, MI 48109, USA
e-mail: mihme@umich.edu

Key words: Large-eddy simulation; Unsteady flamelet modeling; Autoignition

Abstract. *Large-eddy simulation (LES) of a lifted flame in a vitiated co-flow has been performed using an unsteady flamelet/progress variable (UFPV) model. This model is an extension to the steady flamelet/progress variable approach, and describes the transient autoignition process in a lifted flame through the unsteady flamelet model. The particular advantage of this model is that it eliminates the flamelet time scale, and all thermochemical quantities are parameterized by mixture fraction, reaction progress parameter, and stoichiometric scalar dissipation rate. For application to LES, a presumed probability density function closure is employed, in which a beta-distribution is used for the mixture fraction, a statistically most-likely distribution is employed for the reaction progress parameter, and the distribution of the stoichiometric scalar dissipation rate is modeled by a Dirac delta function.*

The UFPV model is applied to LES of a lifted flame in a vitiated co-flow, and simulation results are compared with experimental data and with results obtained from the steady FPV model. Compared to the steady flamelet/progress variable model, predictions from the UFPV model show significant improvements, and the spatial evolution of the flame ignition process and lift-off height are in good agreement with experimental data.

1 INTRODUCTION

The development of advanced combustion systems is mainly controlled by the objective to increase fuel efficiency and to reduce pollutant emissions. To address these issues, novel combustion strategies have been developed, involving the combustion of lean and diluted fuel-air mixtures. Dilution of the fuel-air mixture in internal combustion engines and furnaces is frequently accomplished by recirculating burned gases in order the reduce peak combustion temperature and nitric oxide (NO) emissions. However, despite its enormous potential, combustion of lean and diluted mixtures introduced additional challenges. In particular, the dilution of reactants with inert combustion products can lead to a reduction in the characteristic Damköhler number, so that the reaction kinetics becomes increasingly important. As such, the stability and characteristics of the flame becomes particularly sensitive to variations in fuel composition and operating conditions. Therefore, ignition mechanisms in such flames play a critical role and are directly affected by the turbulence/chemistry interaction.

Autoignition of a fuel mixture in a hot environment is typically initiated in localized regions of low scalar dissipation rate having a mixture composition that favors short ignition times. Since the prediction of autoignition events, however, is strongly dependent on the structure of the surrounding turbulent reacting flow field, combustion models are required that are able to provide an accurate characterization of the spatio-temporal flow field. Although large-eddy simulation (LES) techniques have been demonstrated to provide improved predictions for the turbulent mixing process compared to Reynolds-averaged Navier-Stokes (RANS) approaches,[1] these intermittent ignition events typically occur on scales that are computationally not resolved. Therefore, subgrid scale closure models are required to characterize effects of unresolved scales and ignition kinetics. The objective of this work is to present a LES model for the prediction of autoignition in lifted flames. This model is based on the unsteady flamelet formulation[2] and employs a statistically most-likely probability density function (PDF) as presumed PDF closure model.

The LES autoignition model is applied to a lifted methane/air jet flame, which was experimentally investigated by Cabra *et al.*[3] Gordon *et al.*[4] investigated the transport budget in this flame using a composition PDF approach, and their results indicated that the lifted flame is stabilized by autoignition. Similarly, a joint-scalar transported PDF approach with detailed reaction chemistry coupled with a second moment closure model for the velocity prediction was used by Gkagkas & Lindstedt[5] to compute this lifted flame. Their model reproduced the flow field sensitivity to boundary conditions, and the role of hydroperoxyl and formaldehyde species on the ignition kinetics was characterized. Domingo *et al.*[6] combined a model for autoignition and partially premixed flame propagation. They applied this model to LES of this vitiated flame, and the reported simulation results were in good agreement with experimental data.

Unlike to these model formulations, in the present work a model for the prediction

of autoignition is developed which is based on the unsteady flamelet model for diffusion flames. The mathematical model describing the UFPV formulation and the presumed PDF closure is presented in the next section. The experimental configuration and computational setup are summarized in Sec. 3. Computational results obtained from the model are compared with experimental data and the steady flamelet/progress variable (SFPV) model in Sec. 4. The paper finishes with conclusions.

2 MATHEMATICAL FORMULATION

2.1 Flamelet/Progress Variable Model

For the prediction of autoignition in lifted flames, an unsteady flamelet/progress variable (UFPV) model will be used. In this UFPV model, a flamelet formulation is used to model the structure of the turbulent diffusion flame.[7,8] The unsteady flamelet equations can be written as

$$\frac{\partial \boldsymbol{\phi}}{\partial t} - \frac{\chi_Z}{2}\frac{\partial^2 \boldsymbol{\phi}}{\partial Z^2} = \dot{\boldsymbol{\omega}} \ , \tag{1}$$

where $\dot{\boldsymbol{\omega}}$ corresponds to the source term of all species and temperature, which are collectively denoted by the vector $\boldsymbol{\phi}$. The mixture fraction is denoted by Z, the scalar dissipation rate is

$$\chi_Z = 2\alpha|\nabla Z|^2 \ , \tag{2}$$

and α is the mass diffusivity, which is assumed to be equal for all species. An analytical expression for χ_Z for a counter-flow diffusion flame was derived by Peters.[9] This expression relates χ_Z to its value at stoichiometric condition and a function of Z and $Z_{\rm st}$:

$$\chi_Z = \chi_{Z,\rm st} F(Z; Z_{\rm st}) \ . \tag{3}$$

An unsteady flamelet model, formulated in Lagrangian and Eulerian reference frame, was developed by Pitsch & Steiner[10] and Pitsch.[11] In addition to the local scalar dissipation rate and mixture fraction, this model introduced a local flamelet time that is associated with the convection and diffusion of each flamelet. With this, all thermochemical quantities, $\boldsymbol{\psi} = (\boldsymbol{Y}, T, \nu, \alpha, \dot{\omega}, \dots)^T$, are parameterized in terms of Z, $\chi_{Z,\rm st}$, and t:

$$\boldsymbol{\psi} = \mathcal{E}^{\rm U}_{\boldsymbol{\psi}}(Z, \chi_{Z,\rm st}, t) \ , \tag{4}$$

where $\mathcal{E}_\psi$ denotes the chemistry tabulation and the superscript "U" refers to the unsteady flamelet model. Since this model formulation introduces an explicit dependence on the flamelet time t, it limits its application to canonical flows, in which a flamelet trajectory can be identified. The UFPV model addresses this issue by expressing the flamelet time in terms of the reaction progress parameter Λ and scalar dissipation rate. All thermochemical quantities are then parameterized in the form of

$$\boldsymbol{\psi} = \mathcal{F}^{\rm U}_{\boldsymbol{\psi}}(Z, \Lambda, \chi_{Z,\rm st}) \ . \tag{5}$$

In this UFPV formulation, the flamelet time is replaced by a reaction progress parameter.[12] This mixture-fraction independent parameter, Λ, which is related to the reaction progress variable C, is defined so that each flamelet can be uniquely identified. The reaction progress variable is defined from a linear combination of reaction products as $C = Y_{\mathrm{CO}} + Y_{\mathrm{CO_2}} + Y_{\mathrm{H_2O}} + Y_{\mathrm{H_2}}$, and Λ, having a unique value for each flamelet, corresponds to C evaluated at the stoichiometric condition.[13]

Since expression (5) eliminates the time from the parameterization, it implicitly assumes that the structure of a particular flamelet is independent from its history. In the context of the prediction of radiation and NO pollutant formation it was shown that this is indeed a valid assumption for species that evolve on sufficiently fast time scales.[14] This, however, allows to populate the state space independently from a particular flamelet trajectory. In the present application this is done as follows. First, the S-shaped curve is obtained from the solution of the steady flamelet equations. To obtain solutions 'inside' the S-shaped curve, starting with the initial conditions corresponding to the middle branch or a non-burning flamelet, the unsteady flamelet equations are solved for a specified scalar dissipation rate until the stable solution of the upper branch is reached. If the steady state solution is reached, the process is repeated with a different value for the scalar dissipation until the complete state space is populated.

2.2 Presumed PDF Closure Model

For the LES prediction of turbulent reacting flows, the state relation (5) must be formulated for Favre-filtered quantities. In the following, Favre-filtered thermochemical quantities are computed from Eq. (5) by employing a presumed joint PDF for mixture fraction, reaction progress parameter, and stoichiometric scalar dissipation rate:

$$\widetilde{\boldsymbol{\psi}} = \iiint \mathcal{F}^{\mathrm{U}}_{\boldsymbol{\psi}}(Z, \Lambda, \chi_{Z,\mathrm{st}}) \widetilde{P}(Z, \Lambda, \chi_{Z,\mathrm{st}}) dZ\, d\Lambda\, d\chi_{Z,\mathrm{st}} \ , \tag{6}$$

and $\widetilde{P}(Z, \Lambda, \chi_{Z,\mathrm{st}})$ denotes the density-weighted joint PDF. Since Λ is defined to be statistically independent from Z and $\chi_{Z,\mathrm{st}}$, the conditional PDF $P(\Lambda|Z, \chi_{Z,\mathrm{st}})$ reduces to its marginal PDF. Furthermore, it is assumed that Z and $\chi_{Z,\mathrm{st}}$ are independent. A beta PDF is used to model the mixture fraction distribution,[15,16] and the distribution of $\chi_{Z,\mathrm{st}}$ is modeled by a delta function.[2] A so-called statistically most-likely distribution[17–20] (SMLD) is employed for Λ, so that $\widetilde{P}(Z, \Lambda, \chi_{Z,\mathrm{st}})$ can be written as

$$\widetilde{P}(Z, \Lambda, \chi_{Z,\mathrm{st}}) = \beta(Z; \widetilde{Z}, \widetilde{Z''^2}) \delta(\widetilde{\chi}_{Z,\mathrm{st}} - \chi_{Z,\mathrm{st}}) P_{\mathrm{SML},2}(\Lambda) \ , \tag{7}$$

and

$$P_{\mathrm{SML},j}(\Lambda) = Q(\Lambda) \exp\left\{ \sum_{i=0}^{j} a_i \Lambda^i \right\} \ , \tag{8}$$

where $j = 2$ denotes the number of enforced moments, and $Q(\Lambda)$ is the so-called *a priori* PDF,[21] accounting for bias in composition space. The coefficients a_i, appearing in Eq. (8),

Parameter	Units	Jet	Co-flow
d	m	4.57×10^{-3} $(= D_{\mathrm{ref}})$	0.210
U	m/s	100 $(= U_{\mathrm{ref}})$	5.4
T	K	314	1,355
$X_{\mathrm{O_2}}$	–	0.1452	0.1193
$X_{\mathrm{N_2}}$	–	0.5243	0.7285
$X_{\mathrm{H_2O}}$	–	0.0029	0.1516
$X_{\mathrm{CH_4}}$	–	0.3275	0.0003
$X_{\mathrm{H_2}}$	–	0.0001	0.0001
X_{OH}	–	–	0.0002
Z_{st}	–	0.177	

Table 1: Reference parameters for the lifted jet flame simulation.

are determined by enforcing the first two moments of the reaction progress variable, so that the Favre-filtered thermochemical quantities can be expressed in terms of $\widetilde{C}$ and $\widetilde{C''^2}$. With this, the chemistry table that is used in the UFPV model can then be written in the form:

$$\widetilde{\boldsymbol{\psi}} = \widetilde{\mathcal{G}}^{\mathrm{U}}_{\boldsymbol{\psi}}(\widetilde{Z}, \widetilde{Z''^2}, \widetilde{C}, \widetilde{C''^2}, \widetilde{\chi}_{Z,\mathrm{st}}) \ . \tag{9}$$

In the following, Eq. (9) is used to provide information about all thermochemical quantities in the conservation equations for mass and momentum. In addition to the solution of the Navier-Stokes equations, four addition transport equations for the first two moments of mixture fraction and progress variable are required to close the system of equations in the UFPV model. Details on the modeling of these equations are discussed elsewhere.[22]

3 EXPERIMENTAL CONFIGURATION AND NUMERICAL SETUP

The experiment used for validation of the autoignition model corresponds to the vitiated co-flow burner, which was experimentally studied by Cabra *et al.*[3] The experimental setup consists of a central fuel pipe with a diameter of $D_{\mathrm{ref}} = 4.57$ mm, through which a methane/air mixture at a temperature of 320 K is supplied. The jet exit velocity is $U_{\mathrm{ref}} = 100$ m/s. The Reynolds number based on the fuel nozzle diameter, exit velocity, and kinematic viscosity of the fuel mixture is 24,200, and the value of the stoichiometric mixture fraction is $Z_{\mathrm{st}} = 0.177$. The co-flow consists of reaction products from a premixed hydrogen/air combustion. It is reported that the product mixture, consisting of oxygen, nitrogen, and water, is uniform across the co-flow stream, and the temperature is 1,350 K. The co-flow has a diameter of 210 mm and is surrounded by an exit collar to prevent entrainment of ambient air into the flame. The experimental parameters are summarized in Tab. 1.

The Favre-filtered governing equations are solved in cylindrical coordinates.[23] The geometry is non-dimensionalized by the jet nozzle diameter D_{ref} and the computational domain is $90\, D_{\mathrm{ref}} \times 30\, D_{\mathrm{ref}} \times 2\pi$ in axial, radial, and circumferential directions, respectively.

The axial direction is discretized with 256 grid points following a linear growth rate, and 150 grid points are used in radial direction. The circumferential direction is equally spaced and uses 64 points, resulting in a total number of approximately 2.5 million grid points. The minimum and maximum filter widths are $\Delta_{\rm min} = 4 \times 10^{-2} D_{\rm ref}$ (at the centerline near the nozzle exit) and $\Delta_{\rm max} = 1.27 D_{\rm ref}$ (outermost computational cell at the exit plane).

The turbulent inflow velocity profile was generated from a periodic pipe flow simulation. The unsteady flamelet calculations have been performed using the FlameMaster code,[24] and the chemistry is described by the GRI 2.11 mechanism.[25] From the unsteady flamelets, the UFPV flamelet library is generated. To increase the table resolution, $\widetilde{Z''^2}$ was replaced by the mixedness, $\widetilde{S} = \widetilde{Z''^2}/(\widetilde{Z} - \widetilde{Z}^2)$, and the grid stretching in the directions of $\widetilde{Z}$, $\widetilde{S}$, and $\widetilde{C''^2}$ followed a geometric series. For the discretization of the chemistry table, 75 points are used for the $\widetilde{Z}$ and $\widetilde{C}$ directions, 20 points are used in the directions of $\widetilde{S}$ and $\widetilde{C''^2}$, and 15 points were used for $\widetilde{\chi}_{Z,\rm st}$.

4 RESULTS

4.1 Instantaneous Flow Field

The UFPV model was applied to LES of the Cabra *et al.* flame,[3] and in the following simulation results are compared with experimental data. An additional simulation was conducted using the steady flamelet/progress variable (SFPV) model,[12,23] and differences between both models are discussed. Statistical results, denoted by angular brackets, are obtained from azimuthal and temporal averaging of the instantaneous flow field quantities, and Favre-averaged quantities are computed as $\{\widetilde{\psi}\} = \langle \overline{\rho}\widetilde{\psi}\rangle / \langle \widetilde{\psi}\rangle$.

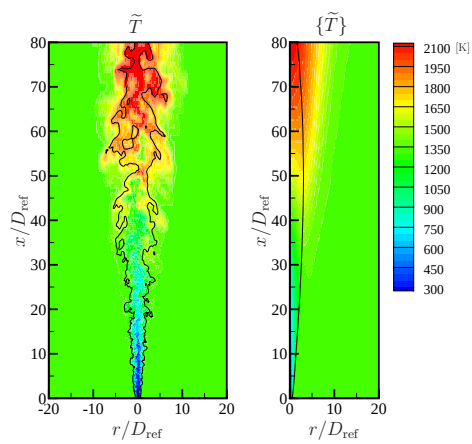

Figure 1: Instantaneous (left) and averaged (right) temperature fields obtained from the UFPV model. The solid line shows the location of stoichiometric mixture fraction.

The instantaneous and averaged temperature fields obtained from the UFPV model are shown in Fig. 1. The solid line in these figures corresponds to the isocontour of the

stoichiometric mixture fraction. From the instantaneous temperature field, obtained from the simulation with the UFPV model, it can be seen that up to approximately $25\,D_{\mathrm{ref}}$ downstream of the jet exit fuel and oxidizer mix without significant heat release. Following this inert mixing zone, a transition region between $30 \leq x/D_{\mathrm{ref}} \leq 50$ is apparent, in which the temperature increases; however, some intermittent pockets with low temperature are evident. Beyond a distance of 50 nozzle diameters above the jet exit the flame is continuously burning, and some entrainment of fluid from the co-flow into the flame core can be observed from the instantaneous flow field results.

4.2 Statistical Flow Field

Favre-averaged results for mixture fraction and temperature along the jet centerline are shown in Fig. 2. Apart from the slight overprediction in the transition region for $25 \leq x/D_{\mathrm{ref}} \leq 60$ the prediction of the mean mixture fraction from the UFPV model is in excellent agreement with the experimental data. The SFPV model considerably overpredicts $\{\widetilde{Z}\}$ in the transition region. The mean temperature from the UFPV model is in overall good agreement with experimental data. The model predicts an initially faster temperature rise in the ignition region, which is further delayed in the downstream direction.

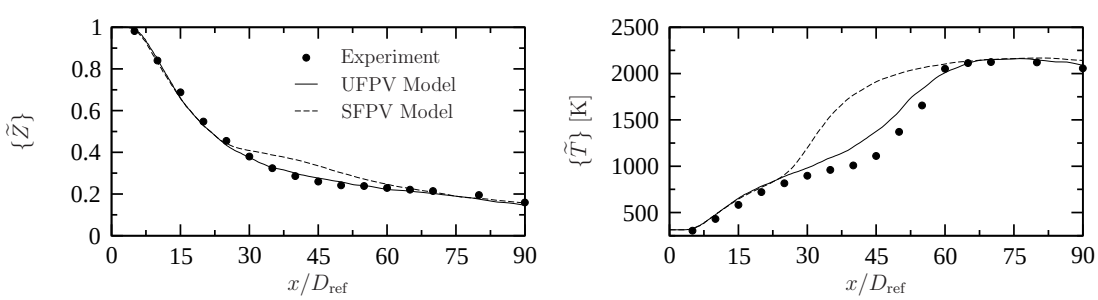

Figure 2: Comparison of measured (symbols) and calculated (lines) mean statistics of mixture fraction and temperature along the centerline for the Cabra-flame.

Radial profiles for mixture fraction, temperature, and species mass fractions of H_2O, CO_2, and CO are compared with experimental data in Fig. 3. Favre-averaged mixture fraction profiles are shown in the first row, and the results from the UFPV model are in better agreement with experimental data compared to the SFPV results. The SFPV model predicts an early flame ignition process, which is not observed in the experimental measurements. Compared to these results, the UFPV model accurately captures the temperature evolution in the transition region; however, the location of the peak temperature is slightly shifted towards the centerline. This discrepancy can be attributed to the overprediction of the mean mixture fraction profiles (see first row) and also to the shortened autoignition, which moves the temperature peak towards fuel-richer composition.

The product mass fractions of H_2O, CO_2 and CO are in similarly good agreement than the temperature profiles, and the spatial evolution of the species is well predicted by the UFPV model.

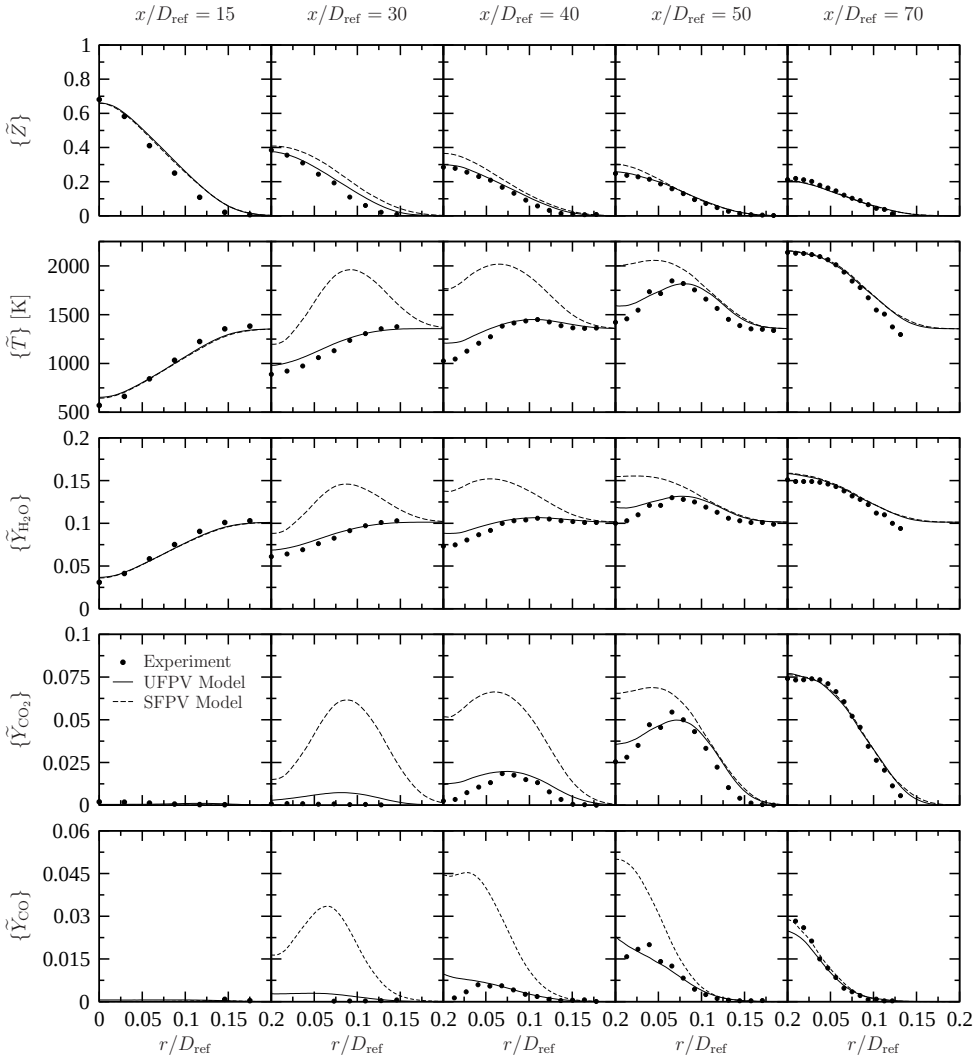

Figure 3: Comparison of radial profiles between simulations and experiments, for mixture fraction, temperature, and species mass fractions of H_2O, CO_2, and CO.

5 CONCLUSIONS

An unsteady flamelet/progress variable model has been applied for the prediction of autoignition in a lifted flame. The model is an extension to the steady flamelet/progress variable approach, and employs an unsteady flamelet model to describe the evolution of all thermochemical quantities during the flame ignition process. In the UFPV model, all

thermochemical quantities are parameterized by mixture fraction, reaction progress parameter, and stoichiometric scalar dissipation rate. The particular advantage of this model over previously developed unsteady flamelet formulations is that in the UFPV model the flamelet time is replaced by physical quantities, which lead to significant simplifications in the computation and parameterization of the thermodynamic state space.

A presumed PDF closure model is employed to evaluate Favre-averaged thermochemical quantities. For this a beta-distribution is used for the mixture fraction, a statistically most-likely distribution is employed for the reaction progress parameter, and the distribution of the stoichiometric scalar dissipation rate is modeled by a Dirac delta function.

The UFPV model was applied to LES of a lifted flame in a vitiated co-flow, and simulation results are compared with experimental data and results obtained from the steady FPV model. Compared to the SFPV model, it is demonstrated that the unsteady formulation leads to significantly improved predictions for flame structure, lift-off height, and spatio-temporal evolution of the flow field. Although the UFPV model predicts a slightly faster ignition behavior, mixture fraction and temperature fields are in good agreement with experimental data.

REFERENCES

[1] H. Pitsch. Large-eddy simulation of turbulent combustion. *Ann. Rev. Fluid Mech.*, 38:453–482, 2006.

[2] H. Pitsch and M. Ihme. An unsteady/flamelet progress variable method for LES of nonpremixed turbulent combustion. *AIAA Paper 2005-557*, 2005.

[3] R. Cabra, J.-Y. Chen, R. W. Dibble, A. N. Karpetis, and R. S. Barlow. Lifted methane-air jet flames in a vitiated coflow. *Combust. Flame*, 143:491–506, 2005. data available from `http://www.me.berkeley.edu/cal/vcb/data/VCMAData.html`.

[4] R. L. Gordon, A. R. Masri, S. B. Pope, and G. M. Goldin. Transport budget in turbulent lifted flames of methane autoigniting in a vitiated co-flow. *Combust. Flame*, 151:495–511, 2007.

[5] K. Gkagkas and R. P. Lindstedt. Transported PDF modeling with detailed chemistry of pre- and auto-ignition in CH_4/air mixtures. *Proc. Combust. Inst.*, 31:1559–1566, 2007.

[6] P. Domingo, L. Vervisch, and D. Veynante. Large-eddy simulation of a lifted methane jet flame in a vitiated coflow. *Combust. Flame*, 152:415–432, 2008.

[7] N. Peters. Laminar diffusion flamelet models in non-premixed turbulent combustion. *Prog. Energy Combust. Sci.*, 10(3):319–339, 1984.

[8] N. Peters. Local quenching due to flame stretch and non-premixed turbulent combustion. *Combust. Sci. Tech.*, 30:1–17, 1983.

[9] N. Peters. *Turbulent Combustion*. Cambridge University Press, Cambridge, 2000.

[10] H. Pitsch and H. Steiner. Large-eddy simulation of a turbulent piloted methane/air diffusion flame (Sandia flame D). *Phys. Fluids*, 12(10):2541–2554, 2000.

[11] H. Pitsch. Improved pollutant predictions in large-eddy simulations of turbulent non-premixed combustion by considering scalar dissipation rate fluctuations. *Proc. Combust. Inst.*, 29:1971–1978, 2002.

[12] M. Ihme, C. M. Cha, and H. Pitsch. Prediction of local extinction and re-ignition effects in non-premixed turbulent combustion using a flamelet/progress variable approach. *Proc. Combust. Inst.*, 30:793–800, 2005.

[13] M. Ihme and H. Pitsch. Prediction of extinction and reignition in non-premixed turbulent flames using a flamelet/progress variable model. 1. A priori study and presumed PDF closure. *Combust. Flame*, 155:70–89, 2008.

[14] M. Ihme and H. Pitsch. Modeling of radiation and NO formation in turbulent non-premixed flames using a flamelet/progress variable formulation. *Phys. Fluids*, 20:055110, 2008.

[15] C. Wall, B. J. Boersma, and P. Moin. An evaluation of the assumed beta probability density function subgrid-scale model for large eddy simulation of nonpremixed, turbulent combustion with heat release. *Phys. Fluids*, 12(10):2522–2529, 2000.

[16] J. Jiménez, A. Liñán, M. M. Rogers, and F. J. Higuera. A priori testing of subgrid models for chemically reacting non-premixed turbulent shear flows. *J. Fluid Mech.*, 349:149–171, 1997.

[17] E. T. Jaynes. Information theory and statistical mechanics. *Phys. Rev.*, 106(4):620–630, 1957.

[18] C. H. Shannon. A mathematical theory of communication. *Bell System Tech. J.*, 27(3):379–423, 1948.

[19] I. J. Good. Maximum-entropy for hypothesis formulation, especially for multidimensional contingency-tables. *Ann. Math. Statist.*, 34(3):911–934, 1963.

[20] S. B. Pope. A rational method of determining probability distributions in turbulent reacting flows. *J. Non-Equilib. Thermodyn.*, 4:309–320, 1979.

[21] C.-S. Fang, J. R. Rajasekera, and H.-S. J. Tsao. *Entropy Optimization and Mathematical Programming*. Kluwer Academic Publisher, Boston, 1997.

[22] M. Ihme and Y. C. See. Prediction of autoignition in a lifted methane/air flame using an unsteady flamelet/progress variable model. *Combust. Flame*, 2009. under review.

[23] C. D. Pierce and P. Moin. Progress-variable approach for large-eddy simulation of non-premixed turbulent combustion. *J. Fluid Mech.*, 504:73–97, 2004.

[24] H. Pitsch. FlameMaster v3.1: A C++ computer program for 0D combustion and 1D laminar flame calculations, 1998. available from `http://www.stanford.edu/group/pitsch/`.

[25] C. T. Bowman, R. K. Hanson, D. F. Davidson, W. C. Gardiner, V. Lissianski, G. P. Smith, D. M. Golden, M. Frenklach, and M. Goldenberg. GRI-Mech 2.11, 1997. available from `http://www.me.berkeley.edu/gri-mech/`.